Zoosyst. Evol. 99 (1) 2023, 63–75 | DOI 10.3897/zse.99.95222

PENSOFT

für Naturkunde MUSEUM FÜR NATURKUNDE BERLIN

Can you find me? A new sponge-like nudibranch from the genus *Jorunna* Bergh, 1876 (Mollusca, Gastropoda, Discodorididae)

Yara Tibiriçá[1,2], Jenny Strömvoll[3], Juan Lucas Cervera[1,2]

1 *Departamento de Biología, Facultad de Ciencias del Mar y Ambientales, Campus de Excelencia Internacional del Mar (CEI·MAR), Universidad de Cádiz, Av. República Saharaui, s/n, 11510 Puerto Real (Cádiz), Spain*

2 *Instituto Universitario de Investigación Marina (INMAR), Campus de Excelencia Internacional del Mar (CEI·MAR), Universidad de Cádiz, Av. República Saharaui, s/n, 11510 Puerto Real (Cádiz), Spain*

3 *Back to Basics Adventures, Ponta do Ouro, Mozambique*

https://zoobank.org/7D011FEE-8B7D-48D5-968A-129CB317B9B2

Corresponding author: Yara Tibiriçá (yara.tibirica@uca.es)

Academic editor: Matthias Glaubrecht ♦ **Received** 22 September 2022 ♦ **Accepted** 9 December 2022 ♦ **Published** 13 January 2023

Abstract

The nudibranch diversity of the western Indian Ocean is comparatively one of the least studied in the world. In this paper a sponge-like Discodoridae nudibranch *Jorunna liviae* **sp. nov.** is described. The description is based on integrative anatomy, including molecular analysis of two genes (the mitochondrial COI and the nuclear H3), dissections, electron microscopy (SEM) of buccal elements, micro tomography of the spicule's arrangements and ecological observations. This study provides the first ever molecular data of *Jorunna* species from the western Indian Ocean, helping to fill the gap to further understand this apparent paraphyletic genus.

Key Words

biodiversity, Heterobranchia, Mozambique, new species, phylogeny, sea slugs

Introduction

The systematic of the genus *Jorunna* was revised by Camacho-García and Gosliner (2008) based on morphological characters. These authors examined 246 specimens (including 30 type specimens) and described two new species. The genus *Jorunna* Bergh, 1876 is widely distributed with species found in the Indo-Pacific, Mediterranean, Atlantic and Eastern Pacific. Alvim and Pimenta (2013) revised the anatomy of the family Discodorididae Bergh, 1891 from Brazil and added a new species for the genus (*Jorunna spongiosa* Alvim & Pimenta, 2013). Recently, Neuhaus et al. (2021) provided a molecular and morphological review of the European species and described a new species (*Jorunna artsdatabankia* Neuhaus, Rauch, Bakken, Picton, Pola & Malaquias, 2021). Currently, 22 *Jorunna* species are accepted as valid (MolluscaBase eds. 2022). Nevertheless, there are still many undescribed species, particularly in the Indo-Pacific. In the field-guide of sea slugs of the Indo-Pacific, Gosliner, Valdés and Behrens (2015) illustrated 16 species of *Jorunna* from which only six are described: *Jorunna funebris* (Kelaart, 1859), *Jorunna labialis* (Eliot, 1908), *Jorunna ramicola* Miller, 1996, *Jorunna rubescens* (Bergh, 1876), *Jorunna parva* (Baba, 1938) and *Jorunna alisonae* Marcus, 1976. Nevertheless, the authors did not include two Australian species: *Jorunna hartleyi* (Burn, 1958) and *Jorunna pantherina* (Angas, 1864).

Despite current research efforts to raise the biodiversity knowledge of nudibranchs from the western Indian Ocean (e.g. Manson-Parker 2015; Tibiriçá et al. 2017a, b, 2018, 2020), this region remains comparatively far less studied than other areas of the Indo-West Pacific. The high number of undescribed species often hampers comprehensive biogeographic studies. Thus, the discovery of new species is of primary importance to advance our global knowledge on how biodiversity is formed and

Copyright *Tibiriçá, Y. et al.* This is an open access article distributed under the terms of the Creative Commons Attribution License (CC BY 4.0), which permits unrestricted use, distribution, and reproduction in any medium, provided the original author and source are credited.

how species diversity spreads across oceans. Moreover, the lack of molecular data from the western Indian Ocean (WIO) limits phylogenetic studies. Of all specimens sequenced from the genus *Jorunna* so far, none are from the WIO. The present study contributes to fill this gap by providing a description of a new *Jorunna* species from Mozambique, including molecular, morphological and ecological data.

Methods

Sample collection

Six specimens were collected by scuba diving in Ponta do Ouro (26°51'26"S, 32°53'4"E), Mozambique by J. Strömvoll & Y. Tibiriçá. All specimens were found on sponge *Amphimedon brevispiculifera* (Dendy, 1905), four on the reef 'Doodles' (26°49'50"S, 32°53'46"E) and two on the 'Steps Reef' (26°49'29"S, 32°53'46"E), between 15–18m depth. Sponge identification was based on a porifera assessment study conducted in the same area (Calcinai et al. 2020). Specimens were photographed *in situ* and in a tank and individually measured. The animals were then relaxed by freezing and preserved in ethanol 96%. Samples were deposited in the Museu Nacional de Ciencias Naturales de Madrid (MNCN) and Museu de História Natural de Maputo (MHNM).

Morphological study

Specimens were dissected by dorsal incision under a dissecting microscope Nikon SMZ18. Their reproductive system was separated, examined and drawn under a dissecting microscope Leica 80 with an attached camera lucida. Surrounding radula tissue was removed by immersing in 10% sodium hydroxide for about 8 hours or on a solution containing 180 mL of the tissue lysis buffer ATL with 20 mL of proteinase K-solution incubated in 56 °C for 48h (Holznagel 1998). Labial cuticle and radula were then mounted for electron microscopy (SEM) examination. Imagines were obtained under a FEI Nano-SEM 450 scanning microscope at the Servicios Centrales de la Ciencia y Tecnlogia de la UCA (MEB), Universidad de Cadiz. Microcomputed tomography (µCT) was carried out to inspect the spicules arrangement by the Servicio de Técnicas No Destructivas del Museo Nacional de Ciencias Naturales de Madrid (MNCN-CSIC). This technique uses x-ray attenuation of biological tissues in three different planes allowing for 2D and 3D image reconstructions (Ziegler et al. 2018). Images were reconstructed using VGSTUDIOMAX 2.2 and visualized in myVGL by Volume Graphics (https://www.volumegraphics.com). Spicules sizes were measured in the µCT images using the distance instrument tool. Measurements were taken from spicules that were clearly visible and from different parts of the body.

DNA extraction, amplification and sequence

DNA extraction and amplification were conducted by the peripheric services of the Instituto Universitario de Investigacion Marina (INMAR–UCA). Genomic DNA was extracted from a small sample of foot tissue using the Qiagen DNeasy Blood & Tissue extraction kit, following the manufacturer's instructions. One mitochondrial gene cytochrome c oxidase subunit (COI) and one nuclear gene histone H3 (h3) were amplified by polymerase chain reaction (PCR), using the universal primers LCO1490 and HCO2198 (Folmer et al. 1994) and H3AD-F and H3BD-R (Colgan et al. 2003), respectively. We tried to amplify the gene 16S using the 16S universal primers 16Sar-L and 16Sbr-H (Palumbi et al. 2002) but all attempts were unsuccessful. PCRs were performed in 25-µl reactions with 2 µl of DNA template. COI amplifications were performed with an initial denaturation for 3 min at 94 °C, followed by 40 cycles of 30 s at 94 °C, 30 s at 46 °C and 1 min at 72 °C with a final extension of 5 min at 72 °C. H3 amplifications were performed with an initial denaturation for 3 min at 95 °C, followed by 25 cycles of 45 s at 94 °C, 45 s at 50 °C (annealing temperature) and 2 min at 72 °C, with a final extension of 10 min at 72 °C. Once completed, successful PCR products were sent to Macrogen, Inc. (Madrid, ES) for purification and sequencing.

All sequences were revised and examined in Geneious v.10.2.4 (Kearse et al. 2012). Possible contamination was verified using the Basic Local Alignment Search tool (BLAST) web server (https://blast.ncbi.nlm.nih.gov/Blast.cgi, Altschul et al. 1990). New sequences were uploaded in Genbank, NCBI and ascension numbers are provided in Appendix 1. Outgroup sequences and other *Jorunna* spp. sequences were obtained from GenBank. The outgroup selection followed Neuhaus et al. (2021). Additionally, one species of each available genus of Discodorididae Bergh, 1891 from GenBank was included in the analysis with preference given for type species. When available, up to three sequences of each morpho-species of *Jorunna* from GenBank, NCBI were included in the phylogeny. Preference was given to specimens with COI and H3. Sequences were aligned in Geneious (https://www.geneious.com) using Muscle and default settings.

Phylogenetic analysis

Maximum likelihood (ML) and Bayesian inference (BI) were used to infer evolutionary relationships. Analyses were conducted for individual genes as well as for the concatenated COI+16S. JModeltest was used to estimate the best fit-evolutionary model by applying the Akaike information criterion (AIC) for each gene. The model chosen was the GTR+I+G for COI and H3. Bayesian inference was performed via MrBayes v.3.2.6 (Ronquist and Huelsenbeck 2003) and run for 5,000,000 generations and four chains, with unlinked parameters, partitioned by genes and a burn-in of 25%. Node support was assessed based on the posterior probability (PP) and considered strongly supported when PP

≥ 0.95 (Alfaro et al. 2003). Maximum likelihood analyses were performed in RAxML v8.2.4 implemented in the Cypres portal, applying 5,000 bootstrap (https://www.phylo.org, Miller et al. 2010). Support for nodes in the ML analysis was assessed with non-parametric bootstrapping (BP) using RAxML v.7.06 (Zhang et al. 2013). Maximum likelihood values of 70 or higher were considered statistically significant (Huelsenbeck and Rannala 2004). The trees obtained were visualized and collapsed (PP ≥ 0.5) in TreeGraph2 (http://treegraph.bioinfweb.info, Stöver and Müller 2010) and edited in Adobe Illustration 2021 v.25.2 (https://www.adobe.com/products/illustrator.html).

Species delimitation

Three molecular species delimitation analyses were conducted to aid the species hypothesis. Firstly, Species by Automatic Partitioning (ASAP) was performed on the in-group COI dataset applying the Kimura two Parameter (K2P) and the default setting parameters (Puillandre et al. 2021). Secondly, the Poisson Tree Processes model (bPTP) was implemented in the bPTP web server (https://species.h-its.org) applying default settings in the COI and concatenated tree resulted from the BI phylogeny (Zhang et al. 2013); and, third, the minimum COI *p*-distance was calculated applying default settings on Mega X version 10.2.4 (Kumar et al. 2018).

Results

Systematics

Order Nudibranchia Cuvier, 1817
Superfamily Doridoidea Rafinesque, 1815
Family Discodorididae Bergh, 1891
Genus *Jorunna* Bergh, 1876

***Jorunna liviae* Tibiriçá, Strömvoll & Cervera, sp. nov.**
https://zoobank.org/5B6809CC-32EE-456F-8302-4B8A3D4E0513

Jorunna sp.: Strömvoll, J. & Jones, G. (2019): pg.49.

Material examined. ***Holotype*:** MNCN15.05/200187 (dissected and sequenced), 12.04.2022, Doodles, Ponta do Ouro, Mozambique, depth 15 m, length 20 mm.

***Paratypes*:** MNCN15.05/200188 (dissected and sequenced), 12.04.2022, Doodles, Ponta do Ouro, Mozambique, depth 17 m, length 11 mm. MNCN15.05/94693 (sequenced and tomography), 12.04.2022, Doodles, Ponta do Ouro, Mozambique, depth 15 m, length 20 mm., size 5 mm. MNCN15.05/200189 (dissected and sequenced), 14.04.2022, Doodles, Ponta do Ouro, Mozambique, depth 18 m, length 13 mm. MHNM.MOL.2022.0002, (2 specs.), 23.06.2022, Steps Reef, Ponta do Ouro, Mozambique, depth 16 m, length 30 mm (both).

Type locality. Ponta do Ouro, Mozambique (26°51'26"S, 32°53'4"E).

Habitat. Specimens were collected on submerged subtropical compressed sandstone reefs in Ponta do Ouro, Mozambique.

Diagnosis. Body elongate-ovulated. Dorsum pale gray to pink, covered on highly dense caryphyllidia; rhinophores short, with up to nine lamellae, ending in a knob apex; six to nine bipinnate branchial leaves encircling the anal pore. Radula with five to seven very thin pectinated outermost teeth bearing long bundled fibrous denticles. Labial cuticle smooth. Copulatory spine with bifid apex.

Etymology. This species is dedicated to Livia Renée Cornelius, daughter of the second author of this paper.

Description. ***External morphology*** (Figs 1, 2). Length varied from 11 to 30mm. Body elongate-ovulated, with gritty texture (Fig. 1A). Mantle covered on highly dense caryophyllid, evenly distributed on the dorsum (Fig. 2A). Caryophyllidia elongated, formed by five to eight spicules, projecting over tip, forming a crown of approximately 140 µm on the dorsum, taller on the margin of gill sheath (≈ 280 µm). Rhinophoral and branchial sheaths low, margin covered by caryophyllidia (Fig. 1D). Rhinophores short, retractable, with six to eight diagonal lamellae with a knob protruding apex (Fig. 1E). Gill with six to nine retractile, bipinnate branchial leaves, held vertically and forming a closed circle around the anal pore (Fig. 1F). Foot narrower than mantle, bilabiate anteriorly, upper lip bifurcate at center (Fig. 1B). Side of the foot covered by spicules (≈ 60 µm), spicules absent on foot sole (Figs 1B, C, 2B, C). Feet do not project beyond mantle in natural crawling position. Oral tentacles small and conical. Dorsum color pale pink to gray. Some specimens covered by pinkish-brown minute dots forming spots distributed on the notum. Gill and rhinophores translucent pinkish-white. Oral tentacle white. Upper lip translucent white with brownish dots. Foot pinkish-white.

***Internal morphology*.** (Figs 3, 4) The visceral mass is enveloped by a translucent-white tissue covered by brownish dots. Eye spots are visible by transparency.

Digestive system. Smooth labial cuticle (Fig. 3A). Oral tube long, about twice the size of oral bulb, with a pair of retractor muscles (Fig. 4A). Buccal bulb ovate, short, radular sac small and ovate, protruding ventrally, with a pair of strong retractor muscles (Fig. 4A).

Radular formula difficult to determinate as outermost teeth are very thin and overlapping each other (Fig. 3B). Approximate radular formula is: 24 × 5–7.22.0.22.5–7 for the 13 mm specimen MNCN15.05/200189 and 38 × 6–7.26.0.26.6–7 for the 20 mm specimen MNCN15.05/200187. Rachidian tooth absent. Innermost and lateral teeth are single cusped, hamate, lacking denticles (Fig. 3C). Lateral teeth gradually increase in size from the inner teeth (≈ 25 µm) toward the external margin (outermost teeth ≈ 100 µm). Five to seven outermost teeth highly differentiated, very thin, pectinate, bearing 5 to 9 long bundled fibrous denticles (Fig. 3D, E).

Oesophagus passing through nerve ring, where it folds. Pair of salivary glands, relatively short, uniform, near the base of oesophagus (4A). Oesophagus connects to oval stomach. Intestine about half of oesophagus diameter. Caecum locate ventrally to stomach.

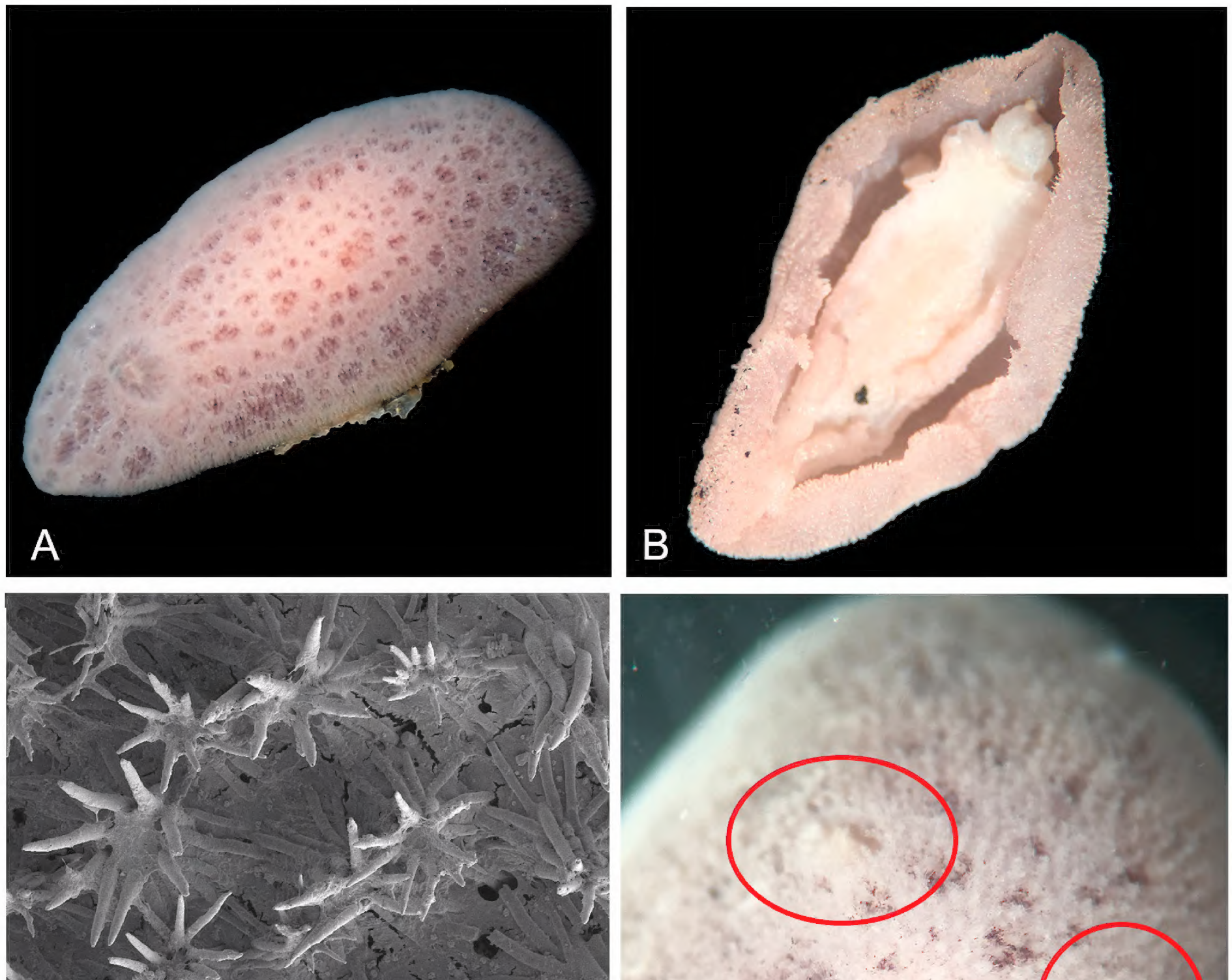

Figure 1. *Jorunna liviae* sp. nov. (MNCN15.05/200187) external morphology. **A.** Dorsal view; **B.** Ventral view; **C.** SEM photography of dorsal caryophyllids; **D.** Rhinophores sheath details; **E.** Rhinophore; **F.** Gill branches.

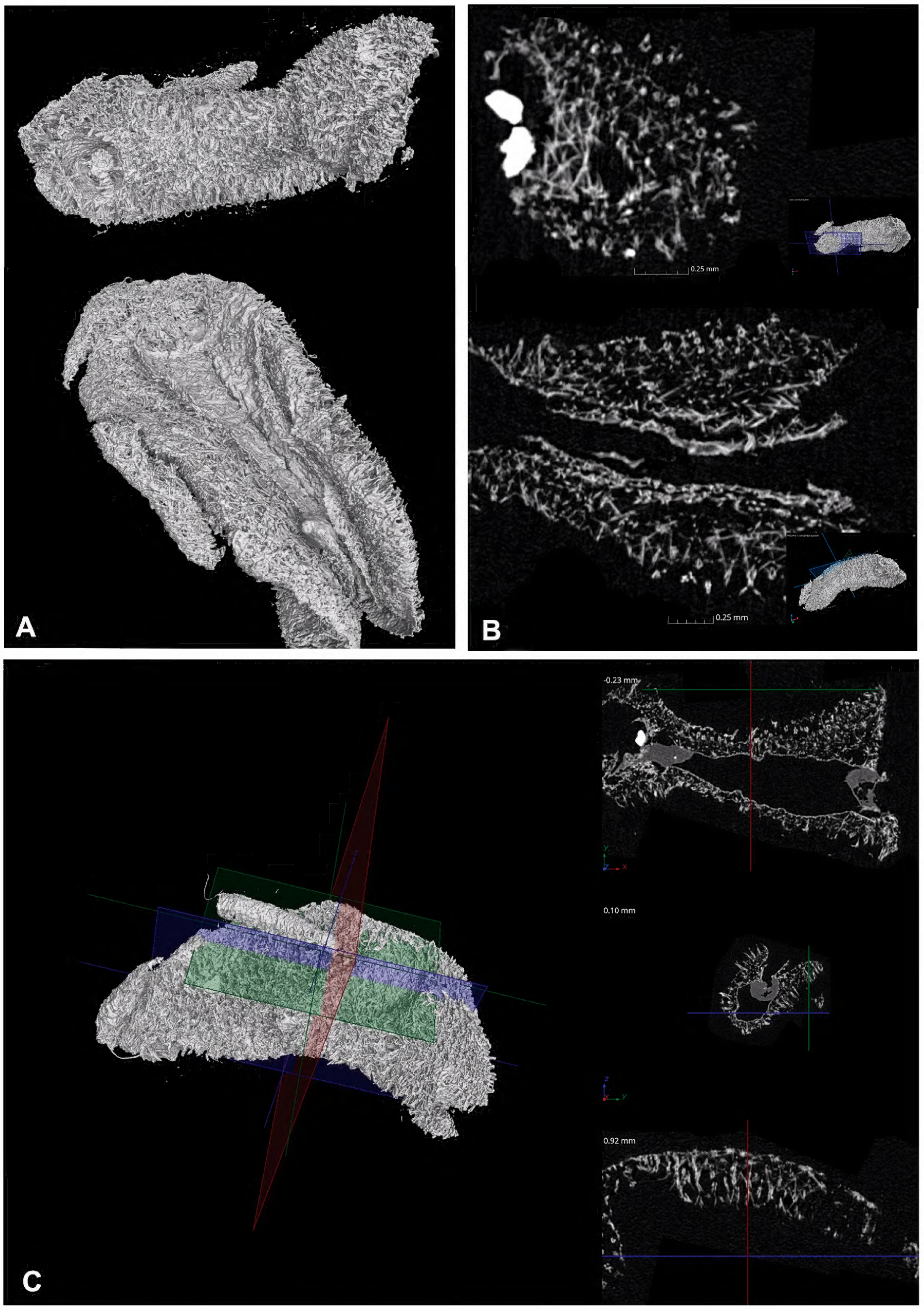

Figure 2. Microcomputed tomography (μCT) of *J. liviae* sp. nov. (MNCN15.05/94693). **A.** Exterior view: dorsal (top) and anterior (bottom); **B.** Internal arrangement of the spicules: dorsal (top) and ventral (bottom); **C.** General internal arrangement of spicules: green = top right; blue = middle right; red = bottom right.

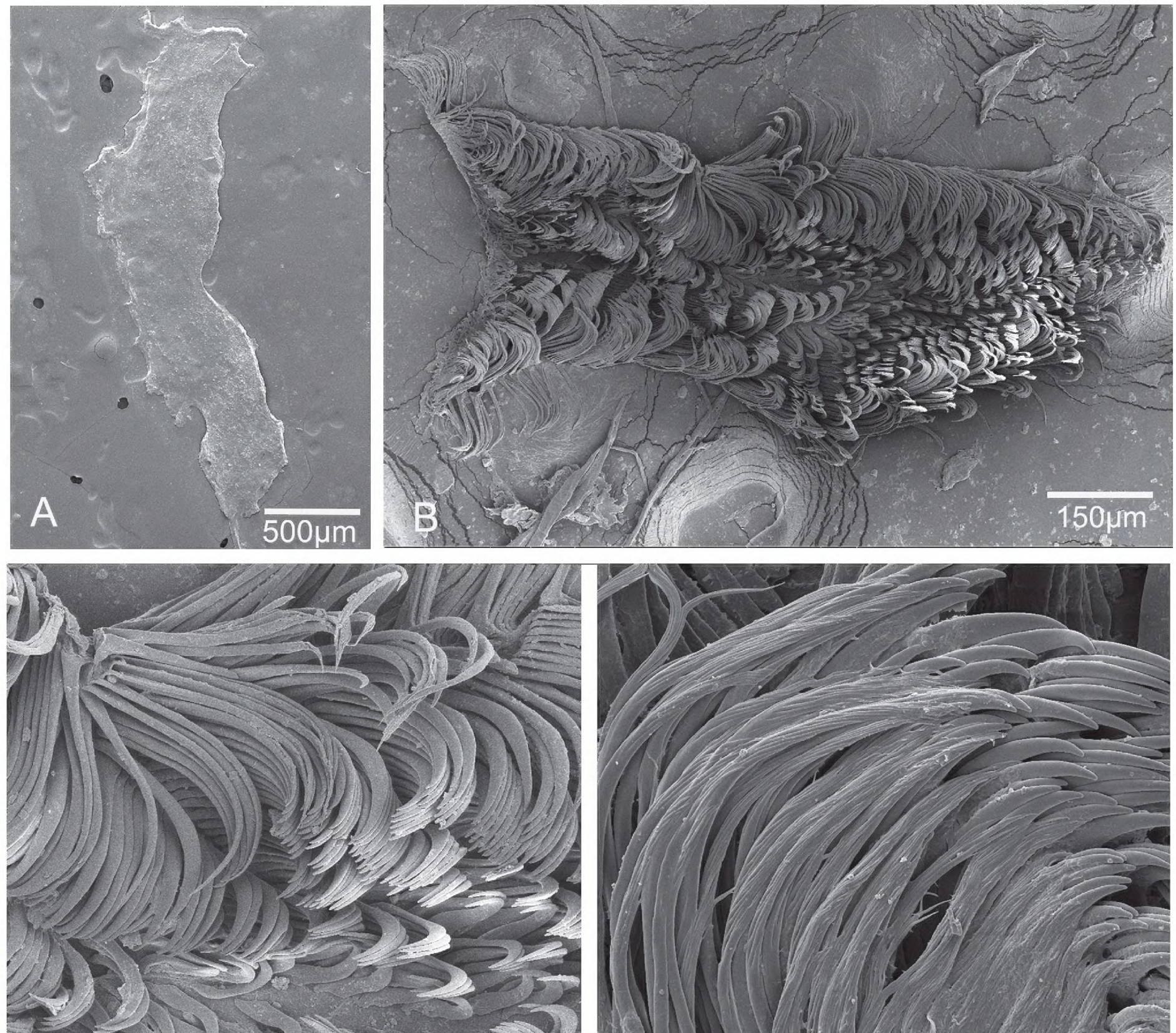

Figure 3. SEM photographs of *Jorunna livae* sp. nov. **A.** labial cuticle (MNCN15.05/200188); **B.** entire view of the radula; **C.** Half-row of posterior part of the radula; **D.** Outermost teeth; **E.** Detail of the outermost teeth; **F.** Copulatory spine.

Digestive gland cone-shaped, occupying approximately 30% of visceral mass. Anus opening at the center of gill circle.

Central nervous system. Central nervous system partially covered by blood gland. This is divided into two parts, anterior part about half the size of posterior part. Cerebral ganglia about half the size of pleural ganglia. Cerebral ganglia and pleural ganglia fused. Pedal ganglia ventrally located connected by a simple pedal commissure. Buccal ganglia short, ventrally located. Rhinophoral ganglia bulb-shaped, about 30% the size of cerebral ganglia. Eyes connected to cerebral gland by short rhinophoral nerve (Fig. 4B).

Reproductive system. Hermaphroditic duct leading to an ampulla long and convoluted, located between female gland and accessory gland. Ampulla branching into short oviduct and prostate. Flattened and ovulated prostate narrowing into a thin deferent duct, expanding into ejaculatory portion. Penis unarmed. Accessory gland size and shape varied according to the specimen, from pear-shaped and similar size to the female gland MNCN15.05/200187 to elongated and half of the size MNCN15.05/200189; in all specimens it narrows into a very thin, highly convoluted tube. Copulatory spine in accessory gland of approximately 1.25 mm (Fig. 3F). Vagina with similar length and width than deferent duct, leading to an oval bursa

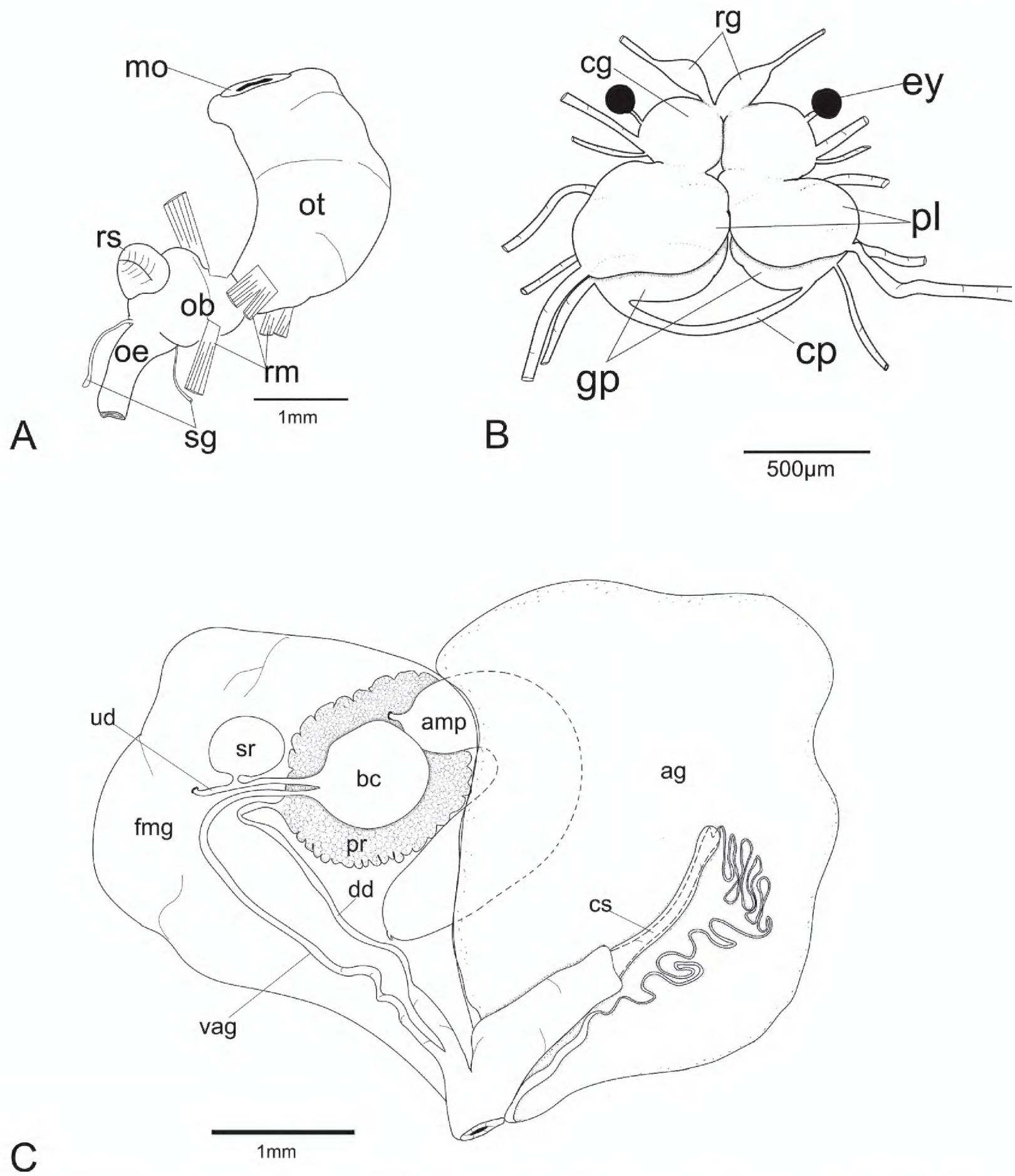

Figure 4. *Jorunna livae* sp. nov. internal anatomy. **A.** Oral mass; **mo** – mouth; rm – retractor muscles; **ob** – oral bulb; **oe** – oesophagus; **ot** – oral tube; **rs** – radular sac; **sg** – salivary gland; **B.** Central system (blood gland removed); **cg** – cerebral ganglia; cp – pedal commissure; **ey** – eye; **gp** – pedal ganglia; **pl** – pleural ganglia; **rg** – rhinophoral ganglia; **C.** Reproductive system; **ag** – accessory gland; **amp** – ampulla; **bc** – bursa copulatrix; **cs** – copulatory spine; **dd** – deferent duct; **pr** – prostate; **sr** – seminal receptacle; **ud** – uterine duct; **vag** – vagina.

copulatrix. Thin duct near the vagina leads to oval seminal receptacle, about 2/3 of the size of the bursa copulatrix, which connects to a large female gland by a short uterine duct (Fig. 4C).

Natural history. This species has only been seen associated with the sponge *A. brevispiculifera*, on which the species is very cryptic (Fig. 5A, B). They are usually found at the base of the sponge branches but they have also been seen on other parts. When removed from the host sponge, the *Jorunna liviae* sp. nov. stretches the body curling the mantle toward the middle of the foot, similar to what Miller (1996) observed for *J. ramicola*. Perhaps this behavior aims to protect the sole of the foot which lacks caryophylliid. The white egg mass is also found on the same sponge and forms a close spiral ribbon of approximately five coils (Fig. 5F). A likely undescribed species of nudibranch egg-eater *Favorinus* sp. has been seen feeding on the *J. liviae* sp. nov. egg mass (Fig. 5C, D). Curiously, most of the time the egg ribbons are found on the tip of the sponge. Perhaps this strategy provides some protection against encrusting organisms due the higher water flux in this part of the sponge. Mating has been observed through July between specimens of different sizes and tonalities (Fig. 5E). *Jorunna liviae* sp. nov. seems to prefer sandy reefs with predominantly hydroids, soft coral and sponges. In Southern Mozambique, the flatter sand reefs have a higher density of sponges than the reefs with predominantly hard coral.

Molecular study and phylogeny. We successfully amplified the gene COI and H3 of four *Jorunna liviae* sp. nov. specimens. The phylogenetic trees constructed by BI and ML analyses of single gene datasets (Suppl. material 1) were not conflictive but differed in the ability to resolve phylogenetic relationships. The single gene H3 analysis retrieved the lowest resolution and the concatenate dataset the highest. Nevertheless, all *Jorunna* species were recovered with more than 50% support in all analysis. In general, the BI analysis better solved the relationship between species, while the ML analysis appears to reflect populational structure. Therefore, the results discussed below are based on the concatenated analysis (Fig. 6), except when stated otherwise.

The family Discodorididae formed a large polytomy. The genus *Jorunna* was divided in two paraphyletic clades, one containing all specimens of *J. funebris* (PP = 1; BS = 94) and another clade with the remaining *Jorunna* species (PP = 0.99; BS = 74).

The COI inter-specific variation (uncorrected *p*-distance) within the genus varied from 9.08% between *J. tomentosa* lineage B (LB) and *J. artsdatabankia* to up 16.92% between *J. funebris* and *J. tomentosa* lineage A (LA) (Table 1). The COI intra-specific variation of *Jorunna liviae* sp. nov. ranged from 0.16% to 1.08%. The closest species to *Jorunna liviae* sp. nov. was *J. tomentosa* lineage B with a minimum *p*-distance of 13.06%. ASAP retrieved 10 partitions, in both analysis (COI and concatenate) the partitions with higher score (asap-score 1.50–3) *Jorunna liviae* sp. nov. was retrieved as a distinct taxonomic unit. Curiously, *J. funebris* were retrieved as a species complex in all possible partitions.

Table 1. COI inter- and intraspecific uncorrected *p*-distances.

	Jorunna artsdatabankia	***Jorunna tomentosa* LA**	***Jorunna tomentosa* LB**	***Jorunna liviae* sp. nov.**	***Jorunna onubensis***	**Intra-specific**
Jorunna artsdatabankia						0–0.15%
Jorunna tomentosa LA	10.30					0.15–0.68%
Jorunna tomentosa LB	9.08	3.65				0.15–0.92%
***Jorunna liviae* sp. nov.**	14.29	14.74	13.06			0.16–1.08%
Jorunna onubensis	12.61	10.74	10.45	12.31		N/A
Jorunna funebris	16.92	17.78	17.78	16.92	16.92	0.46–14.18%

Discussion

The phylogenetic relationships within the family Discodoridae are poorly solved. Most of the type species of Discodoridae genera are not sequenced which hinders our capacity to further understand the family. *Jorunna* is one of the few genera of the Discodoridae family which has its type species (*J. tomentosa*) sequenced. However, a recent study based on three genes (COI+16S+H3) reveals that it is uncertain if *J. tomentosa* represents two distinct lineages (Neuhaus et al. 2021). In our phylogenetic analysis, *J. tomentosa* is divided into two sub-clades (lineage A and B), which form a clade which is sister of *J. artsdatabankia* and related to *J. onubensis* and *J. liviae* sp. nov. Additionally, the genus *Jorunna* appears paraphyletic as *J. funebris* did not nest within the large *Jorunna* clade. In Camacho-García and Gosliner's (2008) morphological study, *J. funebris* nested on a clade together with *J. rubescens*, *J. parva* and *J. pardus*, which is sister of the clade containing the remaining *Jorunna* species studied by the authors. Unfortunately, to date no other species from the *J. funebris* clade has been sequenced. Consequently, the lack of molecular data from several *Jorunna* species hampers any further conclusion about the phylogeny of the genus. Nevertheless, it is clear that the species here described belongs to the genus *Jorunna*, as it forms a clade with the type species. In addition, the new species fits all the morphological diagnosis characters of the genus (see Camacho-García and Gosliner 2008). Interesting, all the species delimitation analyses suggest that *J. funebris* is a species complex, or alternatively, as proposed by Ip et al. (2019), there is an identification error in their sequences.

Jorunna liviae sp. nov. is similar in appearance to the Atlantic species *J. spongiosa* and *J. tomentosa*. This

Figure 5. *Jorunna liviae* sp. nov. *in situ*. **A.** Hosting sponge *Amphimedon brevispiculifera* (Dendy, 1905); **B.** *Jorunna liviae* sp. nov. resting on sponge; **C.** *Jorunna liviae* sp. nov. near its egg mass, and *Favorinus* sp. feeding on it; **D.** Close-up of *Favorinus* sp.; **E.** *Jorunna liviae* sp. nov. mating; **F.** Details of *Jorunna liviae* sp. nov. egg mass.

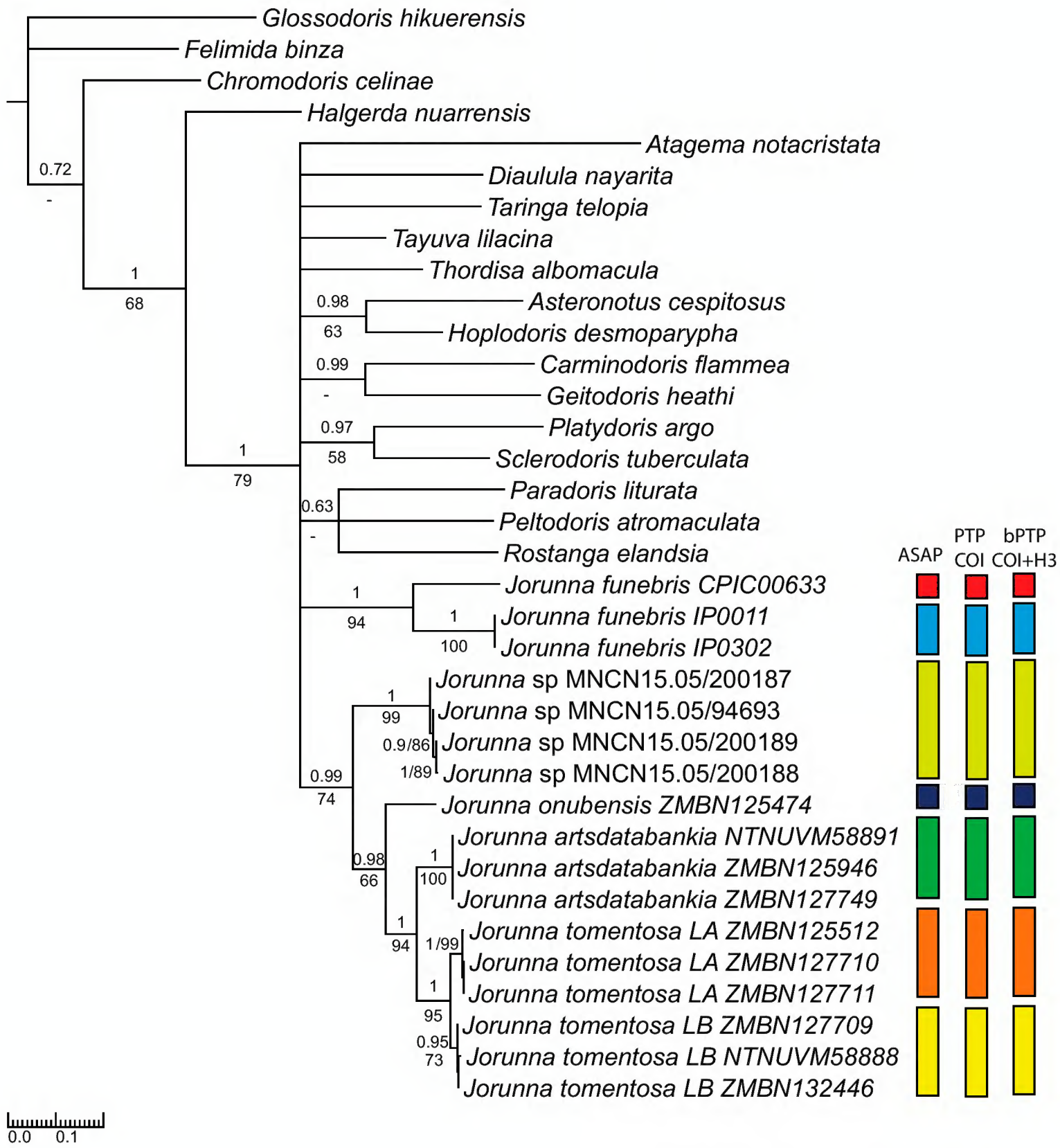

Figure 6. Bayesian inference tree based on the concatenate sequence dataset (COI+H3) collapsed (PP< 0.5). Numbers at the top of nodes indicate Bayesian Posterior probability (PP) and on the bottom bootstrap support from the maximum likelihood analysis (BS). Colored bars on the right represent the results of the species delimitation analyses on the *Jorunna* spp., from left to right: ASAP on COI dataset, PTP on COI dataset, bPTP on COI+H3 dataset.

latter is typically found in European waters (Atlantic and Mediterranean), but few records exist from South Africa and none of them from the Indian Ocean side (Camacho-García and Gosliner 2008; Neuhaus et al. 2021). Apart from the geography and genetic distance, these three species can be clearly distinguished by their radulae, in particular by the shape of the outermost teeth. These are very thin and pectinate in *J. liviae* sp. nov., hooked with small branches on *J. spongiosa* and slender hamate with up to 8 short denticles in *J. tomentosa*. In fact, the outermost pectinate teeth of *Jorunna liviae* sp. nov. are quite unique, and only similar to *J. parva*, a species also found in the WIO but easily distinguishable by the yellow background and dark caryophyllidia. Camacho-García and Gosliner (2008) provided detailed anatomical descriptions and comparative tables of *Jorunna* species by region. To better illustrate the differences between the species described in this study, we adapted and updated Camacho-García and Gosliner's (2008) comparative table of the Indo-Pacific *Jorunna* species, including recent distribution and morphological data observed by us, as well as the species *J. liviae* sp. nov. and *J. labialia* (Table 2). This latter species is found in the western Indian Ocean and Red Sea but was under 'Mediterranean and Western Atlantic' species in Camacho-García and Gosliner's (2008) comparative tables.

The Indo-Pacific species that most resembles *J. liviae* sp. nov. is *J. ramicola*; a species first described from New Zealand and likely occurring in Mozambique (Tibiriçá et al. 2017a). *Jorunna ramicola* is dull in color and bears long, slender outermost teeth which may be described as pectinate. However, these teeth bear much shorter and less numerous denticles, which do not form the distinct bunch as it does in *J. liviae* sp. nov. Moreover, the innermost

Table 2. Comparative morphology of valid *Jorunna* species from the Indo-Pacific Ocean.

	***J. funebris* (Kelaart, 1859)**	***J. pantherina* (Angas, 1864)**	***J. rubescens* (Bergh, 1876)**	***J. parva* (Baba, 1938)**	***J. hartleyi* (Burn, 1958)**	***J. alisonae* Marcus, 1976**	***J. ramicola* Miller, 1996**	***J. labialis***	***J. liviae* sp. nov.**
Geographic range	Indo-Pacific inc. western Indian Ocean	Australia and New Zealand	Indo-Pacific inc. western Indian Ocean	Indo-Pacific inc. western Indian Ocean	Southern Australia	Western and Central Pacific	Indo-Pacific inc. western Indian Ocean	Red Sea & western Indian Ocean	Mozambique
Dorsal color	White to yellow-cream, dark brown rings of different sizes	Purplish brown to pale brown with dark patches	Cream-grey to yellow with oval yellow spots, rings, horizontal black stripes	Dark orange to dark brown, caryophyllidia dark brown	Pale pink, large brown patches encircled with white or dark purple spots	Pale grey, dark grey spots, line of dark spots from rhinophores to gill	Pale grey to light brown with patches of similar color	White to dark dull grey with light brown spots	Pinkish grey, darker spots sometimes present
Rhinophores	14–20 lamellae	16 lamellae, terminal knob	23–25 lamellae	13–15 lamellae	7–8 lamellae	≈ 10 lamellae	short, up to 13 lamellae, terminal knob	wide, 8–11 lamellae	short, 6–8 lamellae, terminal knob
Rhinophore color	White with black apexes	Base colorless, uppermost lamellae speckled in white	Base black or cream-yellow, club black-spotted with white or cream-colored spots	Base light yellow with dark clubs, or dark brown rachises with light yellow clubs	White	Cream-brown with pale grey-brown club	Pale-grey, speckled with dark brown, white on the club	Same than mantle	White to pinkish
Branchial leaves	6 tripinnate	up to 11, bi-tripinnate	6–7, tripinnate	7, bipinnate	10, bipinnate	12, tripinnate	10, bipinnate	11, bipinnate	6–9, bipinnate
Gill color	White with dark black delineations	Same than mantle	Base white, dark brown rachises	Light yellow, base dark brown, tips light-yellow, dark brown rachises	White	Grey to brown with cream glandular spots	Dark grey	?	White to pinkish
Foot sole color	Dark spots around the margin, sole translucent white	Margins sparsely speckled, sole translucent white	Black stripes on sole and laterals, sole white or cream	Dark spots around margin, brown line dorsally, translucent yellow sole	Pink	Pale gray	?	?	Whitish-pink
Upper lip color	White to yellow cream	?	Cream yellow, speckled with black	Yellowish, sometimes with two brown spots on each side of the lip	?	Cream in preserved animals	?	?	White
Oral tentacles color	White to cream, with brown spots in some specimens	Speckled	Light white to yellow	Yellowish	White	Pale gray	?	?	White-pinkish
Caryophyllidia size	≈ 220µm	?	≈ 176µm	≈ 250µm	?	≈ 133µm	≈ 220µm	≈ 190µm	≈ 140µm
Mantle Glands	White, distributed around the mantle edge	?	?	White, large, distributed around the mantle edge	?	Absent	White, distributed around the mantle edge	?	Absent
Foot	Dorsally visible when the animal is in motion	Dorsally visible when the animal is in motion	Dorsally visible when the animal is in motion	Dorsally visible when the animal is in motion	?	Dorsally visible when the animal is in motion	No prolongation present	?	Rarely visible dorsally
Radula	21 × (21.0.21) in 20mm-long preserved specimen	20 × (28.0.28) no more information	26 × (18.0.18) in 18mm specimen	20 × (15.0.15) in 6mm-long preserved specimen	21 × (23.0.23) in 18mm-long preserved specimen	16 × (17.0.17) in 20mm-long preserved specimen	14 × (18.0.18) in 5mm-long preserved specimen	19 × (17.0.17) in 10mm preserved specimen	38 × (6–7.26.0.26.6–7) in 20mm specimen
Innermost teeth	Hamate, shorter and thinner than midlateral teeth, lacking denticles	Hamate, small, lacking denticles	Hamate, blunt, lacking denticles	Hamate, elongated, lacking denticles	Hamate, lacking denticles	Hamate, pointed, shorter than the midlateral teeth, lacking denticles	Hamate, elongate, with up to 3 denticles near the cusp	hamate, single cusp close to base	Hamate, lacking denticles
Midlateral teeth	Hamate, lacking denticles	Hamate, lacking denticles	Elongated, blunt, lacking denticles	Hamate, lacking denticles	Hamate, lacking denticles	Hamate, pointed, lacking denticles	Hamate, pointed, lacking denticles	Hamate, lacking denticles	Hamate, lacking denticles
Outermost teeth	Hamate, lacking denticles	Hamate, lacking denticles	Shorther than midlateral teeth, curved pointed, lacking denticles	Smaller than midlateral teeth. The 5 outermost have up to 5 denticles	Elongated, lacking denticles	Small, elongated, smooth or sometimes with a single denticle near the cusp	elongated, first three outermost teeth with up to 3 denticles	shorter, hamate, pointed	pectinate, 5–8 long fibrous denticles
Labial cuticule	Smooth	With jaw elements	Smooth	Smooth	With jaw elements	With jaw elements	With jaw elements	With jaw elements	Smooth
Accessory gland and spine	Present, curved spine ≈ 717µm long	Present, long pointed spine	Present, curved spine ≈ 3.7mm long	Present, spine ≈ 477µm long	Present, spine ≈ 198µm long	Present, curved spine ≈ 1.03mm long	Present, curved spine ≈ 2.25mm long	Present, curved spine ≈ 600µm long	Present, curved spine ≈ 1.25mm long

teeth in *J. ramicola* are denticulated, while in *J. liviae* sp. nov. they are simple hamate. In addition, the labial cuticle in *J. ramicola* bears jaw elements (Camacho-García and Gosliner 2008), while in *J. liviae* sp. nov. it is smooth. Externally, they can be easily separated by the color of the rhinophores, which in *J. ramicola* is dark pigmented and in *J. liviae* sp. nov. whitish pink. Additional differences are provided in the comparative Table 2.

Conclusions

Based on morphological and genetic data there is no doubt that *J. liviae* sp. nov. is a newly discovered species. Here we provide the first sequence of *Jorunna* species to the WIO. We recommend further efforts to sequence other *Jorunna* species in order to clarify the monophyly of the genus and phylogenetic relationships. In addition, *J. funebris* specimens from different geographic regions should be morphologically and genetically examined as they may represent a species complex.

Acknowledgements

We are grateful to Miguel Gonçales (Park Warden) for assisting with the collection permit. We thank Daniela de Abreu and Alvaro A. Vetina for helping with the deositing of specimens at Museu de História Natural de Maputo (MHNM). We are in great debt to Rupert Cornelius from Back to Basics Adventures for always going out of his way to support research in Ponta do Ouro. We also would like to express our gratitude to Elena Ortega Jimenez and Enrique Gonzales Ortegon (CSIC–ICMAN) for kindly allowing us to use the Nikon SMZ18 for the dissection. Finally, we thank the following technicians for their valuable work: Juan Gonzales (Servicios Centrales de la Ciencia y Tecnologia de la UCA–EB), Cristina Paradela Guerrero (Servicio de Técnicas No Destructivas, MNCN–CSIC) and Francisco Javier Domíngues Marchán (Servicios Periféricos de Biologia Molecular, INMAR–UCA). Molecular, SEM and micro-tomography were supported by funds received by the research group "Marine Biology and Fisheries" PAIDI RNM-213.

References

Alfaro ME, Zoller S, Lutzoni F (2003) Bayes or bootstrap? A simulation study comparing the performance of Bayesian Markov chain Monte Carlo sampling and bootstrapping in assessing phylogenetic confidence. Molecular Biology and Evolution 20(2): 255–266. https://doi.org/10.1093/molbev/msg028

Altschul S, Gish W, Miller W, Myers EW, Lipman DJ (1990) Basic local aligment search tool. Journal of Molecular Biology 215(3): 403–410. https://doi.org/10.1016/S0022-2836(05)80360-2

Alvim J, Pimenta AD (2013) Taxonomic review of the family Discodorididae (Mollusca: Gastropoda: Nudibranchia) from Brazil, with descriptions of two new species. Zootaxa 3745(2): 152–198. https://doi.org/10.11646/zootaxa.3745.2.2

Calcinai B, Belfiore G, Pica D, Torsani F, Palma M, Cerrano C (2020) Porifera from Ponta do Ouro (Mozambique). European Journal of Taxonomy 698: 1–56. https://doi.org/10.5852/ejt.2020.698

Camacho-García YE, Gosliner TM (2008) Systematic revision of *Jorunna* Bergh, 1876 (Nudibranchia: Discodorididae) with a morphological phylogenetic analysis. The Journal of Molluscan Studies 74(2): 143–181. https://doi.org/10.1093/mollus/eyn002

Colgan DJ, Ponder WF, Beacham E, Macaranas JM (2003) Gastropod phylogeny based on six segments from four genes representing coding or non-coding and mitochondrial or nuclear DNA. Molluscan Research 23(2): 123–148. https://doi.org/10.1071/MR03002

Folmer O, Black M, Hoeh W, Lutz R, Vrijenhoek R, Folmer O, Black M, Hoeh W, Lutz R, Vrijenhoek R (1994) DNA primers for amplification of mitochondrial cytochrome c oxidase subunit I from diverse metazoan invertebrates. Molecular Marine Biology and Biotechnology 3: 294–299. https://doi.org/10.1371/journal.pone.0013102

Gosliner TM, Valdés Á, Behrens DW (2015) Nudibranch & Sea Slug Indentification. Indo-Pacific. New World Publications, Inc., Jacksonville, Florida, 408 pp.

Holznagel WE (1998) Research note: A nondestructive method for cleaning gastropod radulae from frozen, alcohol-fixed, or dried material. American Malacological Bulletin 14: 181–183.

Huelsenbeck JP, Rannala B (2004) Frequentist properties of bayesian posterior probabilities of phylogenetic trees under simple and complex substitution models. Systematic Biology 53(6): 904–913. https://doi.org/10.1080/10635150490522629

Ip YCA, Tay YC, Gan SX, Ang HP, Tun K, Chou LM, Huang D, Meier R (2019) From marine park to future genomic observatory? Enhancing marine biodiversity assessments using a biocode approach. Biodiversity Data Journal 7: e46833. https://doi.org/10.3897/BDJ.7.e46833

Kearse M, Moir R, Wilson A, Stones-Havas S, Cheung M, Sturrock S, Buxton S, Cooper A, Markowitz S, Duran C, Thierer T, Ashton B, Meintjes P, Drummond A (2012) Geneious Basic: An integrated and extendable desktop software platform for the organization and analysis of sequence data. Bioinformatics 28(12): 1647–1649. https://doi.org/10.1093/bioinformatics/bts199

Kumar S, Stecher G, Li M, Knyaz C, Tamura K (2018) MEGA X: Molecular evolutionary genetics analysis across computing platforms. Molecular Biology and Evolution 35(6): 1547–1549. https://doi.org/10.1093/molbev/msy096

Manson-Parker C (2015) Nudibranchs of Seychelles. Archipelago Images 2015, 32 pp. http://www.archipelagoimages.net

Miller MC (1996) The dorid nudibranch genus *Jorunna* Bergh, 1876 (Gastropoda: Opisthobranchia) in New Zealand. Journal of Natural History 30(7): 1095–11009. https://doi.org/10.1080/00222939600770591

Miller MA, Pfeiffer W, Schwartz T (2010) Creating the CIPRES Science Gateway for inference of large phylogenetic trees. In: Proceeding of the Gateway Computing Environments Workshop, 1–8. https://doi.org/10.1109/GCE.2010.5676129

MolluscaBase eds. (2022) WoRMS taxon details. *Jorunna* Bergh, 1876. World Register of Marine Species. MolluscaBase. https://www.marinespecies.org/aphia.php?p=taxdetails&id=138098

Neuhaus J, Rauch C, Bakken T, Picton B, Pola M, Malaquias MAE (2021) The genus *Jorunna* (Nudibranchia: Discodorididae) in Europe: A new species and a possible case of incipient speciation. The Journal of Molluscan Studies 87(4): eyab028. https://doi.org/10.1093/mollus/eyab028

Palumbi SR, Martin A, Romano S, McMillan WO, Stice L, Grabowski G (2002) The simple fool's guide to PCR version 2. University of Hawaii 96822: 1–45. https://doi.org/10.1186/s13620-015-0060-3

Puillandre N, Brouillet S, Achaz G (2021) ASAP: Assemble species by automatic partitioning. Molecular Ecology Resources 21(2): 609–620. https://doi.org/10.1111/1755-0998.13281

Ronquist F, Huelsenbeck JPP (2003) MRBAYES 3, Bayesian phylogenetic inference under mixed models. Bioinformatics 19(12): 1572–1574. https://doi.org/10.1093/bioinformatics/btg180

Stöver BC, Müller KF (2010) TreeGraph 2: Combining and visualizing evidence from different phylogenetic analyses. BMC Bioinformatics 11(1): 1–9. https://doi.org/10.1186/1471-2105-11-7

Tibiriçá Y, Pola M, Cervera JL (2017a) Astonishing diversity revealed: an annotated and illustrated inventory of Nudipleura (Gastropoda: Heterobranchia) from Mozambique. Zootaxa 4359(1): 1–133. https://doi.org/10.11646/zootaxa.4359.1.1

Tibiriçá Y, Pola M, Cervera JL (2017b) Two new species of the genus *Aldisa* Bergh, 1878 (Gastropoda, Heterobranchia, Nudibranchia) from southern Mozambique. Marine Biodiversity 49: 43–56. https://doi.org/10.1007/s12526-017-0752-x

Tibiriçá Y, Pola M, Cervera JL (2018) Systematics of the genus *Halgerda* Bergh, 1880 (Heterobranchia : Nudibranchia) of Mozambique with descriptions of six new species. Invertebrate Systematics 32(6): 1388–1421. https://doi.org/10.1071/IS17095

Tibiriçá Y, Pola M, Ortigosa D, Cervera JL (2020) Systematic review of the "*Chromodoris quadricolor* group" of East Africa, with descriptions of two new species of the genus *Chromodoris* Alder & Hancock, 1855 (Heterobranchia, Nudibranchia). Journal of Zoological Systematics and Evolutionary Research 58(1): 230–261. https://doi.org/10.1111/jzs.12334

Zhang J, Kapli P, Pavlidis P, Stamatakis A (2013) A general species delimitation method with applications to phylogenetic placements. Bioinformatics 29(22): 2869–2876. https://doi.org/10.1093/bioinformatics/btt499

Ziegler A, Bock C, Ketten DR, Mair RW, Mueller S, Nagelmann N, Pracht ED, Schröder L (2018) Digital three-dimensional imaging techniques provide new analytical pathways for malacological research. American Malacological Bulletin 36(2): 248–273. https://doi.org/10.4003/006.036.0205

Appendix 1

Table A1. List of specimens used in the molecular analysis with respective sample localities, voucher number and GenBank accession numbers.

Species	Locality	Voucher	COI	H3
Jorunna artsdatabankia	Norway: Frøya	NTNU-VM-58891	MW784174	MW810589
Jorunna artsdatabankia	Norway: North Sea	ZMBN 125946	MW784173	MW810590
Jorunna artsdatabankia	Norway: Kristiansund	ZMBN 127749	MW784172	–
Jorunna funebris	Guam: Mariana Islands	CPIC00633	KP871645	KP871669
Jorunna funebris	Sister Islands: Singapore	IP0011	MN690306	–
Jorunna funebris	Sister Islands: Singapore	IP0302	MN690307	–
Jorunna tomentosa lineage A	Norway: Gulen	ZMBN 127710	MW784177	MW810611
Jorunna tomentosa lineage A	Northern Ireland: Ballyhenry Is. Northern	ZMBN 127711	MW784180	MW810603
Jorunna tomentosa lineage A	France: La Rochelle	ZMBN 125512	MW784175	MW810597
Jorunna tomentosa lineage B	Norway: Frøya	NTNU-VM-58888	MW784204	MW810600
Jorunna tomentosa lineage B	Northern Ireland: Ballyhenry Island	ZMBN 127709	MW784190	MW810594
Jorunna tomentosa lineage B	Spain: Pontevedra, Galicia	ZMBN 132446	MW784193	MW810599
Jorunna onubensis	Spain: Huelva	ZMBN 125474	MW784171	MW810587
Jorunna liviae sp. nov.	Mozambique: Ponta do Ouro	MNCN15.05/200189	OP948384	OP939409
Jorunna liviae sp. nov.	Mozambique: Ponta do Ouro	MNCN15.05/200187	OP948382	OP939411
Jorunna liviae sp. nov.	Mozambique: Ponta do Ouro	MNCN15.05/200188	OP948383	OP939410
Jorunna liviae sp. nov.	Mozambique: Ponta do Ouro	MNCN15.05/94693	OP948385	OP939412

Supplementary material 1

Bayesian maximum credibility tree of the COI and 16S sequence alignments for *Jorunna liviae* sp. nov.

Authors: Yara Tibiriçá, Jenny Strömvoll, Juan Lucas Cervera
Data type: phylogenetic
Explanation note: Bayesian maximum credibility tree of the COI and 16S sequence alignments. Posterior probabilities (PP) are indicated above each and bootstrap values (BS) are indicated below each branch. Branch lengths indicates the proportion of substitutions. PP< 0.5 and BS< 50 are not shown.
Copyright notice: This dataset is made available under the Open Database License (http://opendatacommons.org/licenses/odbl/1.0/). The Open Database License (ODbL) is a license agreement intended to allow users to freely share, modify, and use this Dataset while maintaining this same freedom for others, provided that the original source and author(s) are credited.
Link: https://doi.org/10.3897/zse.99.95222.suppl1

Supplementary material 2

Table of locality

Authors: Yara Tibiriçá, Jenny Strömvoll, Juan Lucas Cervera
Data type: occurences
Explanation note: Table of locality of collected specimens of *Jorunna liviae* sp. nov.
Copyright notice: This dataset is made available under the Open Database License (http://opendatacommons.org/licenses/odbl/1.0/). The Open Database License (ODbL) is a license agreement intended to allow users to freely share, modify, and use this Dataset while maintaining this same freedom for others, provided that the original source and author(s) are credited.
Link: https://doi.org/10.3897/zse.99.95222.suppl2